Structural Performance of Degraded Reinforced Concrete Members

J. I. Braverman[1], C. A. Miller[1], B. R. Ellingwood[2], D. J. Naus[3], C. H. Hofmayer[1], P. Bezler[1], and T.Y. Chang[4]

1) Brookhaven National Laboratory, Upton, NY
2) School of Civil & Environmental Engineering, Georgia Institute of Technology, Atlanta, GA
3) Oak Ridge National Laboratory, Oak Ridge, TN
4) U.S. Nuclear Regulatory Commission, Washington, D.C.

ABSTRACT

This paper describes the results of a study to evaluate, in probabilistic terms, the effects of age-related degradation on the structural performance of reinforced concrete members at nuclear power plants. The paper focuses on degradation of reinforced concrete flexural members and shear walls due to the loss of steel reinforcing area and loss of concrete area (cracking/spalling). Loss of steel area is typically caused by corrosion while cracking and spalling can be caused by corrosion of reinforcing steel, freeze-thaw, or aggressive chemical attack. Structural performance in the presence of uncertainties is depicted by a fragility (or conditional probability of failure). The effects of degradation on the fragility of reinforced concrete members are calculated to assess the potential significance of various levels of degradation. The fragility modeling procedures applied to degraded concrete members can be used to assess the effects of degradation on plant risk and can lead to the development of probability-based degradation acceptance limits.

INTRODUCTION

All commercial nuclear power plants (NPPs) contain concrete structures whose performance and function are necessary to protect the safety of plant operating personnel and the general public. Although these structures are passive under normal operating conditions, they play a key role in mitigating the impact of extreme environmental events such as earthquakes, high winds, and tornadoes. The past performance of reinforced concrete structures in NPPs has been good, with the majority of the problems identified during construction and corrected at that time. However, as these structures age, incidences of degradation due to various aging mechanisms are likely to increase the potential threat to their functionality and durability. Some evidence of this has been reported in Ashar and Bagchi, 1995; Naus et al., 1999; and Braverman et al., 2000. Incidences of degradation have been identified in intake structures/pumphouses, tendon galleries, masonry walls, anchorages, containments, and other concrete structures, often in areas exposed to water, aggressive chemicals, or freeze-thaw cycling.

Concrete structural components, such as shear walls, slabs, beams and columns, that are found in the reactor building, control or auxiliary building, and other balance-of-plant facilities, are designed and constructed in accordance with criteria in ACI Standards 318, 349, and the NRC Standard Review Plan 3.8.4. Such components generally have substantial safety margins when properly designed and constructed; however, the available margins for aged or degraded concrete structures are not known. Aging can lead to changes in engineering properties and may affect the dynamic properties, structural resistance/capacity, failure mode, and location of failure initiation. This paper discusses the research effort performed to evaluate the effects of degradation of reinforced concrete flexural members and shear walls found in U.S. NPPs.

FRAGILITY METHODOLOGY

Degradation effects can be quantified with fragility curves developed for both undegraded and degraded components. Fragility analysis is a technique for assessing, in probabilistic terms, the capability of an engineered system to withstand a specified event. Fragility modeling requires a focus on the behavior of the system as a whole and, specifically, on things that can go wrong with the system. The fragility modeling process leads to a median-centered (or likely) estimate of system performance, coupled with an estimate of the variability or uncertainty in performance. The fragility concept has found widespread usage in the nuclear industry, where it has been used in seismic probabilistic safety and/or margin assessments of safety-related plant systems (Kennedy and Ravindra, 1984).

The lognormal cumulative distribution function (CDF), is the most common model in structural fragility analysis. If the structural capacity is described as the product of statistically independent random variables, the central limit theorem provides some justification for the lognormal model. The lognormal CDF is described by,

$$F_R(x) = \Phi\,[\ln(x/m_C)/\beta_C] \qquad (1)$$

in which $F_R(x)$ is the probability of failure for an applied load equal to x, $\Phi\,[\,]$ = standard normal probability integral, m_C = median capacity, and β_C = logarithmic standard deviation, approximately equal to the coefficient of variation, V_C, when $V_C < 0.3$. It should be emphasized that all sources of uncertainty known to impact structural performance should be included in this model. These would include aleatory uncertainties, β_R (inherent variability in strength of concrete and reinforcing steel,

dimensions, etc) and epistemic uncertainties, β_U (simplifying assumptions regarding structural mechanics, approximate methods of analysis, limitations in data). There are a number of ways to distinguish between these sources of uncertainty in the fragility assessment. In this study, we combine the aleatory and epistemic uncertainties as, $\beta_C = \sqrt{\beta_R^2 + \beta_U^2}$ in Eq. (1).

A summary of available statistical data to describe the strength of reinforced concrete flexural members (beams and slabs) and short concrete shear wall structures is provided in Tables 1 and 2, respectively. These are based on a comprehensive review of published literature (Ellingwood and Hwang, 1985; MacGregor et al., 1983) and additional data from specific NPPs. The limit state for the beams considered herein is defined by the beam strength measured in terms of uniform load capacity. Deformation-based limit states (peak displacement, maximum rotations, or ductility) usually are not the limiting condition for flexural members in NPPs. Most loads acting on flexural members in power plants are static gravity loads, with dynamic seismic loads constituting a small portion of the total load. Thus, static rather than dynamic effects are considered for the beam. Since the principal loads acting on the flexural members are considered to be static, the steel and concrete strengths presented are static strengths in-situ, i.e., the strength when loading to failure takes approximately one hour. Mill tests of steel and concrete cylinder tests are conducted at a higher strain rate than is typical for static structural loading, and must be adjusted to static conditions. The principal loads acting on shear walls, however, are generally due to seismic so that dynamic concrete and steel properties are used. This accounts for the differences in the data in Tables 1 and 2. The in-situ strength of concrete requires additional corrections to account for differences between standard-cure cylinder strengths and field strengths that arise from field placement, consolidation, and curing conditions (MacGregor, et al., 1983). Thus, the concrete strength statistics reflect 28-day in-situ strength under static load conditions for the flexural members and under dynamic load conditions for the shear walls. There can be a significant gain in concrete strength beyond the 28-day strength used as the basis for design. Such increases have only a nominal effect on flexural strength of the under-reinforced beam, but may have a substantial impact on shear wall behavior, where the concrete strength is more important. For conservatism, this strength increase is ignored in the current study.

Table 1
Structural Resistance Statistics for Beams

Property	Mean	V_C	CDF
Concrete (4,000 psi)			
Comp. Strength	3,552 psi	0.16	N
Splitting strength	358 psi	0.18	N
Initial tangent modulus	3,800 ksi	0.18	
Max comp. strain	0.004	0.20	N
Grade 60 reinforcement			
Yield strength	66 ksi	0.10	LN
Modulus of Elasticity	29,000 ksi	NA	
Placement of reinforcement			
Effective depth, d	d (in)	0.5/d	N
Analysis Flexure (B_f)	1.04	0.07	N

Note: 1 in. = 25.4 mm; 1 psi = 6.895 kPa; 1 ksi = 6.895 MPa;
N = normal distribution; LN = lognormal distribution

Table 2
Structural Resistance Statistics for Shear Walls

Property	Mean	V_C	CDF
Concrete (4,000 psi)			
Comp. Strength	4,400 psi	0.16	N
Splitting strength	475 psi	0.18	N
Initial tangent modulus	3,834 ksi	0.18	
Max comp. strain	0.004	0.20	N
Grade 60 reinforcement			
Yield strength	71 ksi	0.10	LN
Modulus of Elasticity	29,000 ksi	NA	
Placement of reinforcement			
Effective depth, d	d (in)	0.5/d	N
Analysis Shear (B_{sh})	1.00	0.14	N

Note: 1 in. = 25.4 mm; 1 psi = 6.895 kPa; 1 ksi = 6.895 MPa;
N = normal distribution; LN = lognormal distribution

The factors B_f and B_{sh} account for epistemic uncertainty in the analysis itself. This uncertainty arises from idealizations of behavior in any analytical model of a structure. Refined structural models (e.g., nonlinear FEA) tend to be closer to reality than design code models, and in such cases the means of B_f or B_{sh} will be close to 1 (unbiased).

The uncertainties are propagated through the analyses of the structural components using Latin Hypercube sampling, a stratified sampling technique designed to reduce the variance in the estimator for small samples. Nineteen samples are used for each analysis to facilitate probability plotting within approximately the center 90% range of the fragility curve.

FRAGILITY EVALUATION OF DEGRADED FLEXURAL MEMBERS

Degradation effects on the behavior of indeterminate flexural reinforced concrete members are determined using a specific example of a propped cantilever beam. Fragility curves for the undegraded beam and the beam with degraded properties are calculated and compared for varying levels of degradation. Lognormal distributions for the important beam properties are developed both for the undegraded and degraded conditions. These properties are then used to evaluate the probability of failure for the beam. Extensive calculations are performed with an analytical model of the beam (as recommended in ACI 318) and these results are verified with a finite element model of the beam.

Beam Design and ACI Code Analysis

A propped cantilever beam with a 6.1 meter (20 ft) span is used as the sample problem. The beam is designed, using the procedures in ACI 318-99, for a dead load of 14.6 kN/m (1 kip/ft) and a live load of 43.8 kN/m (3 kips/ft). The resulting ultimate load on the beam (including load factors) is 94.9 kN/m (6.5 kips/ft). The design of the beam used compressive strength of concrete (f'_c) at 27.6 MPa (4,000 psi) and Grade 60 reinforcement [yield strength f_y = 414 MPa (60 ksi)]. Young's modulus for the concrete is 24.9 GPa (3,605 ksi). The design is shown in Fig. 1. The reinforcement ratios in the negative and positive moment regions are 0.0145 and 0.0087, respectively. The balanced reinforcement ratio is 0.0285 so that one expects the strength of the beam to be controlled by yielding of the reinforcement as required in the Code.

The load-deflection behavior of the beam is evaluated using the procedures defined in ACI 318. When the loading is small and before concrete cracking occurs, the stiffness of the beam is controlled by the gross section with negligible contribution from the reinforcement. The bending moment causing cracking (M_{cr}) is defined in the ACI code to occur when the tensile flexural stress is $f_r = 7.5\ [f'_c]^{1/2}$ = 474 psi (3.27 MPa). The value of M_{cr} is 66.8 kN-m (49.3 ft-kips). The maximum bending moment occurs at the fixed support and is equal to $w L^2 / 8$. Equating this moment to the cracking moment results in the cracking load [w_{cr} = 14.4 kN/m (0.986 kips/ft)]. The ultimate moment capacities of the beam, evaluated at the support and positive moment regions are M_u^- = 490 kN-m (361 ft-kips) and M_u^+ = 312 kN-m (230 ft-kips), respectively. The first plastic hinge occurs at the support when the loading equals 105 kN/m (7.22 kips/ft). The second plastic hinge occurs at 3.81 m (12.5 ft) from the fixed support when the load equals 114 kN/m (7.79 kips/ft). The magnitude of this load is:

$$w_u = 2\ [M_u^- + M_u^+ L / (L - x)] / L\ x \qquad (3)$$

where x is the location of the second plastic hinge which is 3.81 m (12.5 ft) from the support.

Finite Element Model

The results from the above closed form solutions are verified with a finite element model of the beam with solutions obtained using the ANSYS computer code. The model used for the beam is shown in Fig. 2. The concrete is modeled with element "SOLID65" of ANSYS. Cracking and crushing behavior of the concrete is considered in the solutions. The steel reinforcement is modeled discretely with spar elements having elastic-perfectly plastic material properties.

The uniform load on the beam is increased until convergence of the ANSYS solutions can no longer be achieved. Cracking is calculated to occur at a load of 24.1 kN/m (1.65 kips/ft). The first plastic hinge (defined at the first yielding of the reinforcement) forms at 103 kN/m (7.05 kips/ft) and the second plastic hinge forms at 115 kN/m (7.88 kips/ft). It should be recalled that the corresponding ACI code calculated values are 14.4 kN/m (0.986 kips/ft) for cracking, 105 kN/m (7.22 kips/ft) for the first plastic hinge, and 114 kN/m (7.79 kips/ft) for the second hinge. Plots of load versus deflection for the beam are shown in Fig. 3 for both the finite element and hand calculation models. It can be seen that the agreement between the two is quite good. Based on these results, the ACI 318 calculations are used to generate the beam fragility curves.

Fragility Results for Beams

Fragility curves are generated for the undegraded (benchmark case) and degraded beams. The data presented in Table 1 are used to develop the fragility of the undegraded beam. Equation (3) is used to evaluate the beam strength for each of 19 Latin Hypercube samples. A standard statistical package is used to evaluate the 19 samples and the resulting mean strength is found to be 126 kN/m (8.66 kips/ft) (compared to 114 kN/m (7.79 kips/ft) for the design case). The logarithmic standard deviation, V_C, is found to be 0.11.

Based on published data, several levels of corrosion were identified for crack widths observed in concrete members. It was found that crack (parallel to the reinforcement) widths on the order of 0.15 mm (0.0059 in.) correspond to the first stage of corrosion with essentially no reduction in steel area or bond strength, while crack widths on the order of 9 mm (0.354 in.) are associated with 20% loss in steel (cross-sectional) area and significant loss of bond strength. Since the 9 mm (0.354 in.) crack would be readily observable during an inspection and would afford the opportunity to make repairs, it was decided to consider steel area losses of 20% and 10% (treated as random variables). The 20% reduction in steel area is modeled with a mean steel area of 4.05 cm^2 (0.628 sq. in.) (the original area of the 25.4 mm [# 8] bar is 5.1 cm^2 [0.79 sq. in.]) with a COV in area equal to 0.07 while the 10% reduction in steel area is modeled with a mean steel area equal to 4.55 cm^2 (0.706 sq. in.) and a COV equal to 0.05.

In addition to loss of steel area, concrete spalling (resulting from either freeze thaw problems or steel corrosion) is also considered as a degradation mechanism in this study. Spalls in concrete beams usually occur outside of the steel cage. This is modeled by reducing the effective depth of the beam section by subtracting the cover from the depth. The cover is defined with a mean depth of 4.45 cm (1.75 in.) with a COV in depth equal to 0.36. Since corrosion can result in loss of steel and concrete spalling, the combined case of both effects are considered in addition to the individual effects.

The fragility parameters for the degraded beam are summarized in Table 3. The distributions are also shown in Fig. 4. The results indicate that there is about ½% probability of failure at the design ultimate capacity of 94.9 kN/m (6.5 kips/ft). It can be seen (in the Table and Figure) that the V_C is about the same for all cases and thus the fragilities are nearly parallel to

one another. The strength of the beam is reduced by less than 18% for the worst cases. The most severe cases result from a 20% loss of steel area. It should be noted that this mechanism is associated with severe cracking of the concrete section which could be readily observed during an inspection. It is believed that inspections of the facility would identify such problem areas before serious degradation of strength occurs. The results for the beam evaluation have been expanded to other beams and slabs and are presented in NUREG/CR-6715 (Braverman et al., 2001).

Table 3
Fragility Curve Statistics for Degraded and Undegraded Beam Case

Case	Mean Capacity		V_C
	(kips/ft)	(kN/m)	
Undegraded	8.66	126	0.11
Bottom Spall	8.23	120	0.12
Top Spall	8.06	118	0.12
Top and Bottom Spall	7.89	115	0.13
10% Loss of Top and Bottom Steel	7.81	114	0.12
20% Loss of Top and Bottom Steel	7.29	106	0.13
20% Loss of Steel & Spall, Both at Bottom	7.11	104	0.12
20% Loss of Steel & Spall, Both at Top	7.45	109	0.12

FRAGILITY EVALUATION OF DEGRADED SHEAR WALLS

Validation of Analytical Code

A series of tests performed in Japan (Yamakawa, 1995) on shear walls are used to verify ANSYS models of shear walls. The walls are 950 mm (37.4 in.) high, 800 mm (31.5 in.) wide, and 80 mm (3.15 in.) thick. The reinforcement consists of two layers of 6 mm bars (0.236 in.) spaced at 100 mm (3.94 in.) in each direction. Thick (essentially rigid) edge beams were placed at the top and bottom of the specimen. Static cyclic loading was applied to the specimens. Both undegraded and degraded (with various levels of steel corrosion) shear walls were tested; the verification is made for the undegraded case.

The ANSYS model used for this verification study utilizes the finite element "SOLID65" which includes both cracking and crushing of the concrete. The development of a crack at an integration point modifies the stress-strain relations by introducing a plane of weakness. The post-cracking behavior is represented using a shear transfer coefficient which consists of a shear strength reduction factor for subsequent loads which induce sliding (shear) across the crack face. The shear transfer coefficient can range from 0.0 to 1.0. A value of 0.5 was selected for this study and varied by ± 25% to evaluate its impact. The sensitivity analyses indicated that the response of the model was not significantly affected by variation in this parameter. The steel reinforcement is modeled with elastic-perfectly plastic spar elements.

A comparison of the load-deflection behavior and crack patterns from the test specimens and the ANSYS model demonstrated that the ANSYS finite element modeling approach is suitable for predicting the behavior of reinforced concrete shear walls for the purpose of this study.

Deterministic Analyses of a Representative Shear Wall

A specific shear wall with characteristics that are representative of those found in NPPs, illustrated in Fig. 5, was selected to evaluate the effects of degradation on reinforced concrete walls. The wall is 6.1 m (20 ft) high by 6.1 m (20 ft) wide and is 61 cm (2 ft) thick. The reinforcement consists of 15.9 mm (#5) bars spaced at 21.6 cm (8.5 in.) at each face in each direction resulting in a horizontal and vertical reinforcing ratio equal to 0.003. The shear wall is assumed to be part of an enclosure of a square room having similar shear walls on all sides and a ceiling with similar dimensions. The walls normal to the shear wall under consideration act as flanges and provide moment resistance. The ceiling slab acts as a stiff member to distribute the shear load uniformly across the wall. A vertical load resulting from gravity loads in the building is included and selected to produce a uniform compressive stress in the wall equal to 2.07 MPa (300 psi). The specified concrete strength is taken as 27.6 MPa (4 ksi) and grade 60 reinforcement is used. Several analytical methods are used to calculate the ultimate capacities for comparison with the ANSYS solution.

ACI Design Code Methodology

Using ACI 318-99 the shear capacity of the wall can be calculated using the expression:

$$\phi V_n = \phi \left[3.3 \left(f'_c\right)^{1/2} h\, d + N_u\, d / 4\, L_w + A_v\, f_y\, d / s_2\right] \quad (4)$$

where, ϕ = capacity reduction factor, taken =1.0 (since true estimate of capacity is desired for fragility calculations)

h = wall thickness; $d = 0.8 * \text{wall width}$

A_v = area of horizontal steel within distance s_2; s_2 = spacing of horizontal reinforcement

N_u = axial load = $0.3 * h * L_w$; L_w = wall width

The resulting design capacity of the wall in shear is calculated to be 2,150 kips (9.56MN).

Barda et al. Methodology

The ACI code is known to be conservative for low-rise walls. Barda et al. (1977) used experimental data (based on tests of low-rise shear walls) to develop the following equation for the concrete contribution to the wall shear strength:

$$V_{conc} = [8.3\,(f'_c)^{1/2} - 3.4\,(f'_c)^{1/2}\,(H / L_w - 0.5) + N_u /(4\,h\,L_w)]\,h\,d; \quad \text{where, } H = \text{wall height} \qquad (5)$$

For fragility analyses, in which the statistics of V_{conc} are required, the term $f_t / 6$ (where f_t = splitting strength) should be substituted for $(f'_c)^{1/2}$. This is necessary because the variability in the shear strength is incorrectly reduced when $(f'_c)^{1/2}$ is used in Eq. (5). To account for the contribution of vertical and horizontal reinforcement to wall strength, Wesley and Hashimoto (1981) developed the following equation for the shear strength developed from the horizontal and vertical reinforcement ratios (ρ_h and ρ_v):

$$V_{steel} = [a\,\rho_h + b\,\rho_v]\,f_y\,h\,d \qquad (6)$$

where, $a = 1 - b$

$b = 1$ for $H / L_w < 0.5$; $= 2\,(1 - h / L_w)$ for $0.5 < H / L_w < 1$; $= 0$; for $H / Lw > 1$

The total shear wall capacity is calculated as the sum of equations (5) and (6). This results in a shear capacity of 3,170 kips (14.1 MN), which is about 50% higher than the ACI code predicted capacity.

Evaluation of Shear Wall (Design Case) Using Finite Element Method

The ANSYS model used to evaluate the load-deflection characteristics of the example wall is shown in Fig. 6. The same model characteristics are used as discussed above for the ANSYS validation except that the material properties reflect the design properties. The material properties used for this "design case" are f'_c = 27.6 MPa (4 ksi), f_t = 3.09 MPa (448 psi), E_{it} (initial tangent modulus) = 26.4 GPa (3,834 ksi), and f_y = 414 MPa (60 ksi). Sensitivity studies were made for various solution parameters (load step size, number of iterations, and convergence criteria) to confirm the accuracy of the selected values while minimizing the computer execution time. Several sensitivity studies were also conducted to determine the importance of certain design and analysis parameters. The studies included variations on the concrete tensile strength and the shear transfer coefficient used as input for the ANSYS finite element when cracking occurs. Based on the results of these studies and past experience, the values selected for these parameters would provide reasonable results for this model.

A load-deflection plot derived from the ANSYS solution is shown in Fig. 7. Straight lines are fit to the elastic and inelastic portion of the design curve so that various characteristics of the curve may be established. This shows that the yield load is about 2,550 kips (11.3 MN) and the corresponding yield deflection is 0.075 in. (1.91 mm) (drift ratio = 0.03%). The limit state is defined as the drift ratio equal to four times the yield drift ratio, a point where significant damage to attachments and penetrations may occur. Similar limiting deformation levels have been assumed in previous seismic PRAs and margin studies of NPPs (e.g., Wesley and Hashimoto, 1981). For the "design case" shown in Fig. 7, the limit state is calculated to be 0.3 in. (7.62 mm).

Recall that the ACI Code and Barda et al. methodology predicted wall strengths are 2,150 kips (9.56 MN) and 3,170 kips (14.1 MN), respectively. These are shown in Fig. 7. It can be seen that the ACI Code predicted strength is about 83% of the yield load while the Barda et al. methodology predicted strength results in a deflection equal to approximately 0.18 in. (4.57 mm) (2.3 times yield deflection).

Fragility Results for Shear Walls

The same shear wall model shown in Fig. 6 is used to develop fragility curves for evaluation of the effect of degradation. The data shown in Table 2 are used to develop fragility data for the shear wall. A horizontal lateral (in plane) load is applied to the top of the wall for each case and increased until large plastic deformations occur. The wall is evaluated using an equivalent static lateral force method of analysis, making the process of evaluation of wall capacity similar to a nonlinear pushover analysis of the type often used in recent years to evaluate buildings for earthquake resistance. The objective of the study is to develop the relative fragilities for undegraded and degraded concrete members. It is likely that dynamic effects play similar roles in modifying the fragilities for both conditions, and therefore the ratio of the degraded to undegraded fragility would be about the same in either case. Load-deflection curves are calculated for the 19 sample data for the undegraded case and each degraded condition. For each curve, straight lines are fitted to the elastic and plastic portions of the curve (similar to those shown in Fig. 7 for the design case). Then the load corresponding to 4 times the design yield drift is read off the curve.

Solutions are obtained for both the undegraded wall and for degradation of the wall with a 20% loss of steel area and complete spalling of the concrete cover. The solutions for the undegraded case indicate a mean strength of 16.3 MN (3,655 kips) with a V_C of 0.15. Solutions for the 20% steel area loss indicate a mean strength of 16.2 MN (3,634 kips) with a V_C equal to 0.16. Considering a 20% loss of steel area in combination with concrete spalling, the mean strength is reduced further to 15.3 MN (3, 446 kips) with a coefficient of variation equal to 0.15. A plot of the fragility curves is given in Fig. 8. For this case, the 20% loss of steel area was considered only for the shear wall (i.e., not the flange walls).

To confirm the fragility results for the shear wall by analytical means is difficult. It is known that applying the ACI code methodology to low rise shear walls leads to very conservative (i.e. low) estimates of ultimate shear load capacity. Therefore, the Barda et al. methodology is used to determine the effect of degradation on the ultimate capacity (not the deformation-related limit state as defined previously for this study). For the configuration and design studied in this paper, the resulting mean strength (ultimate shear capacities) for the undegraded case is calculated to be 16.7 MN (3,751 kips). For the 20% loss of steel area the means strength is 15.8 MN (3,545 kips) and for the combined loss of steel area and concrete spalling the mean strength drops to 14.4 MN (3,244 kips). These results, as well as the finite element evaluation, indicate that the effect of degradation due to loss of steel (up to 20%) is small. This occurs because of the relatively low steel ratio for the sample shear wall problem. Evaluation of the wall for other variations in degradation and design parameters (e.g., different reinforcement ratios and aspect ratios) are presented in NUREG/CR-6715.

CONCLUSIONS

The evaluation of degraded reinforced concrete flexural members and shear walls considered in this research has lead to the following conclusions:

1. For a 20% loss of steel cross-sectional area (without concrete spalling) or complete spalling of concrete cover (without loss of steel area) the strength of degraded beams decreases by less than 20%. For the case of loss of steel area in combination with complete concrete spalling, the loss of steel area must be restricted to be less than 20% in order to maintain the same level of reduction in fragility curves.
2. Beam fragility curves shift to lower values of strength and remain almost parallel to each other as the beam properties degrade. This implies that the effects of degradation on beam strength at any given conditional probability of failure can be estimated, to first approximation, by considering the impact of degradation on its median capacity, determined by assuming all parameters take on their median values.
3. Finite element results for the shear wall, having an aspect ratio of 1.0 and a steel ratio of 0.003, indicate that the effect of a 20% loss of steel area in combination with spalling of concrete results in a reduction of the mean wall strength of approximately 6%. The effects of steel degradation increase for higher steel ratios and larger aspect ratios.
4. As in the case of flexural members, the wall fragility curves shift to lower values of strength and remain nearly parallel when degradation occurs. Therefore, the effects of degradation can be estimated, to first order, by determining the median capacity from the medians of the individual variables, and anchoring the reduced fragility curves at the 50^{th} percentile.
5. The research effort also assessed the potential effects of degradation on plant risk and developed probability-based degradation acceptance limits. Details of this are presented in NUREG/CR-6715.

REFERENCES

1. Ashar, H. and Bagchi, G. (1995). "Assessment of Inservice Conditions of Safety-Related Nuclear Power Plant Structures." NUREG-1522. U. S. Nuclear Regulatory Commission, Washington, D.C.
2. Naus, D. J., Oland, C. B., Ellingwood, B. R., Hookham, C. J., and Graves, H. L. (1999). "Summary and Conclusions of a Program to Address Aging of Nuclear Power Plant Concrete Structures." Nuclear Engineering and Design, 194 (1999): 73-96.
3. Braverman, J. I., et al., (2000). "Assessment of Age-Related Degradation of Structures and Passive Components for U.S. Nuclear Power Plants." NUREG/CR-6679. Brookhaven National Laboratory, Upton, N.Y.
4. ACI 318. "Building Code Requirements for Reinforced Concrete." American Concrete Institute, Farmington Hills, Michigan.
5. ACI 349. "Code Requirements for Nuclear Safety Related Concrete Structures." American Concrete Institute, Farmington Hills, Michigan.
6. NRC "Standard Review Plan for the Review of Safety Analysis Reports for Nuclear Power Plants." NUREG-0800. U.S. Nuclear Regulatory Commission, Washington, D.C.
7. Kennedy, R. P. and Ravindra, M., (1984), "Seismic Fragilities for Nuclear Power Plant Studies." Nuclear Engineering and Design 79(1): 47-68.
8. Ellingwood, B. R. and Hwang, H., (1985), " Probabilistic Descriptions of Resistance of Safety-Related Structures in Nuclear Plants." Nuclear Engineering and Design 88(2): 169-178.
9. MacGregor, J. G., Mirza, S. A. and Ellingwood, B. R., (1983). "Statistical Analysis of Resistance of Reinforced and Prestressed Concrete Members." Journal American Concrete Institute 80 (3): 167-176.
10. ANSYS. Finite Element Computer Code. ANSYS Rev. 5.4, ANSYS, Inc., Canonsburg, PA.
11. Braverman, J. I., Miller, C. A., Ellingwood, B. R., Naus, D. J., Hofmayer, C. H., Shteyngart, S., and Bezler, P., (2001). "Probability-Based Evaluation of Degraded Reinforced Concrete Components in Nuclear Power Plants." NUREG/CR-6715. Brookhaven National Laboratory, Upton, N.Y. (to be published in early 2001)

12. Yamakawa, T., (1995), "An Experimental Study on Deterioration of Aseismic Behavior of R/C Structural Walls Damaged by Electrolytic Corrosion Testing Method." Concrete Under Severe Conditions: Environment and Loading, Volume 2, Edited by K. Sakai, N. Banthia and O.E. Gjorv, E & FN Spon, London, England.
13. Barda, F., Hanson, J. M., and Corley, W. G., "Shear Strength of Low-Rise Walls with Boundary Elements," Reinforced Concrete Structures in Seismic Zones, ACI SP-53, American Concrete Institute, 1977.
14. Wesley, D. A., and Hashimoto, P. S. "Seismic Structural Fragility Investigation for the Zion Nuclear Power Plant." NUREG/CR-2320. U.S. Nuclear Regulatory Commission, October 1981.

DISCLAIMER

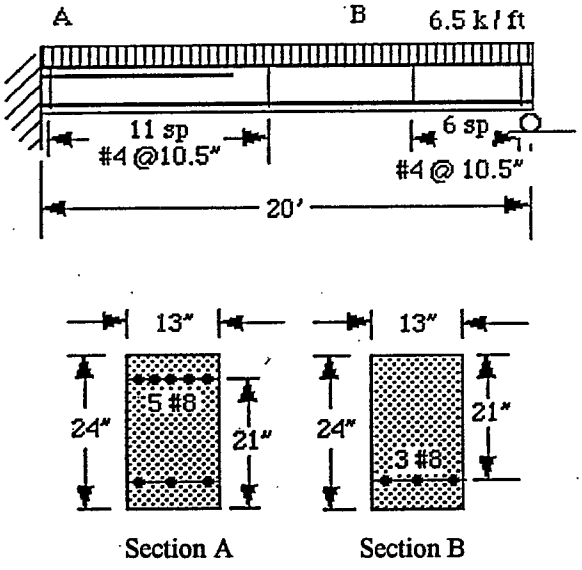

Fig. 1 Sample Beam Problem
(1 in. = 25.4 mm; 1 ft = 30.48 cm; 1 kip/ft = 14.6 kN/m)

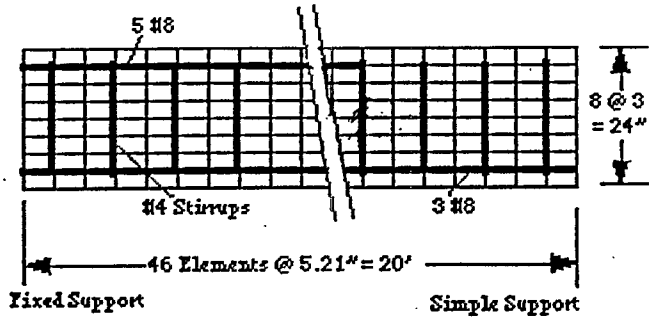

Fig. 2 ANSYS Beam Model
(1 in. =25.4 mm; 1 ft = 30.48 cm)

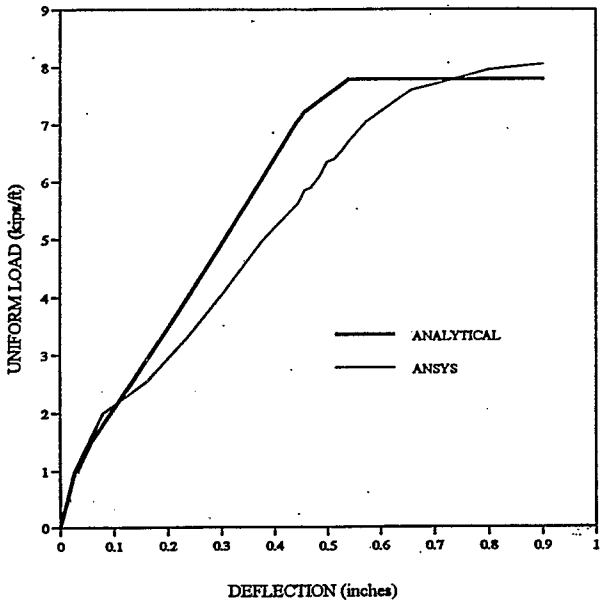

Fig. 3 Comparison of ANSYS and Analytical Beam Deflection Prediction (1 in. = 25.4 mm; 1 kip/ft = 14.6 kN/m)

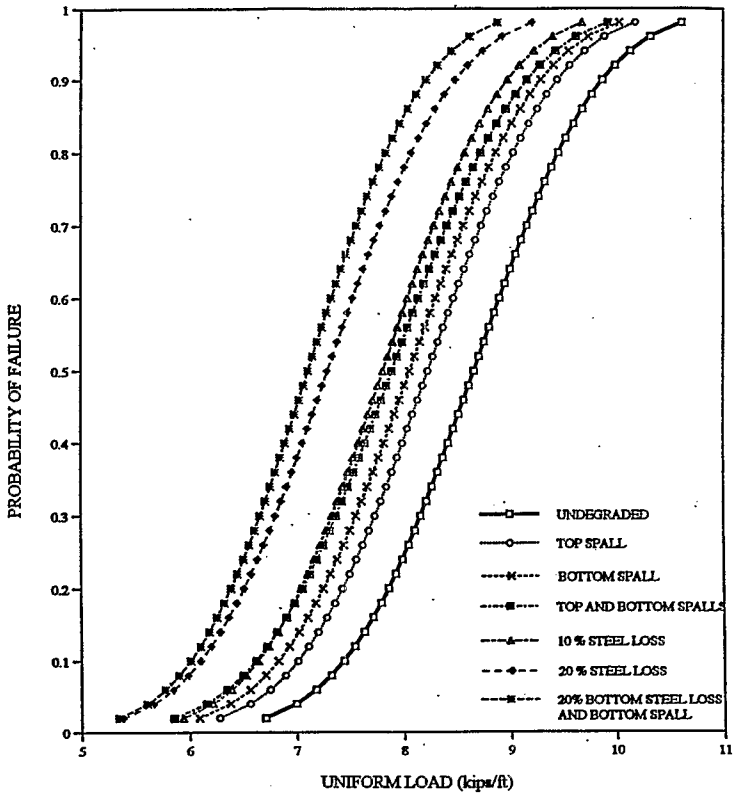

Fig. 4 Effects of Degradation on Beam Strength
(1 kip/ft = 14.6 kN/m)

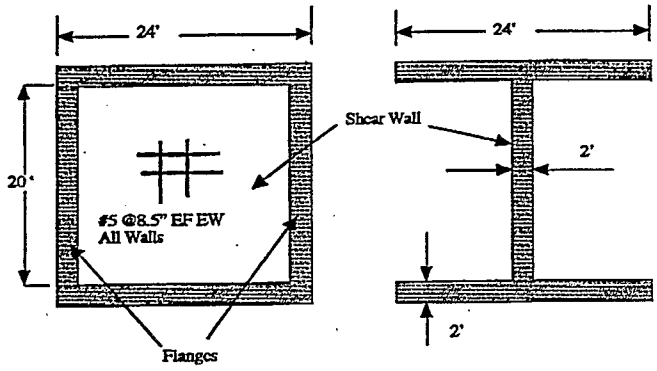

Fig. 5 Example Problem Shear Wall Design
(1 in. = 25.4 mm; 1 ft = 30.48 cm)

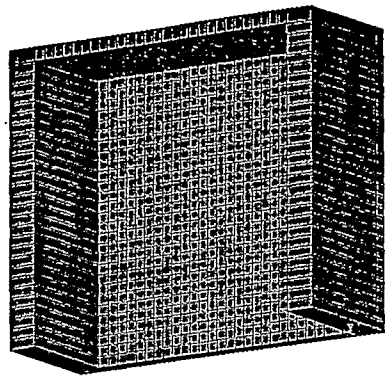

Fig. 6 Sample Shear Wall – Finite Element Model

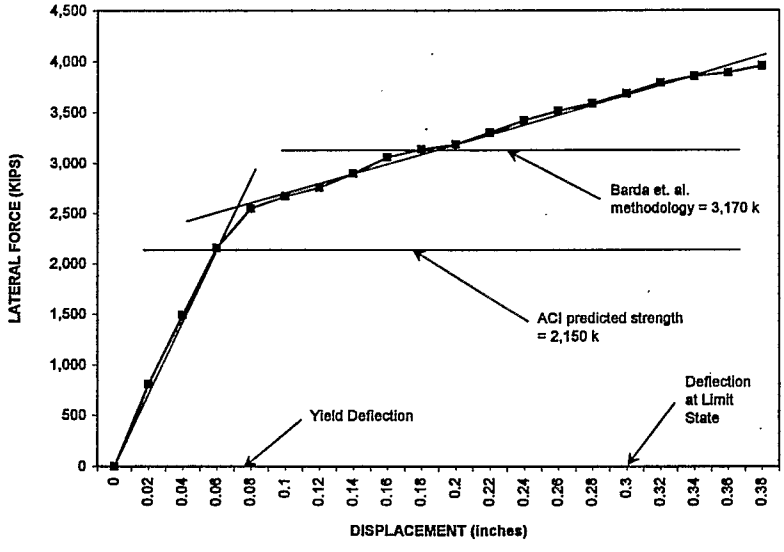

Fig. 7 Shear Wall Design Case – Undegraded Load-Deflection Curve (1 in. = 25.4 mm; 1 kip = 4.45 kN)

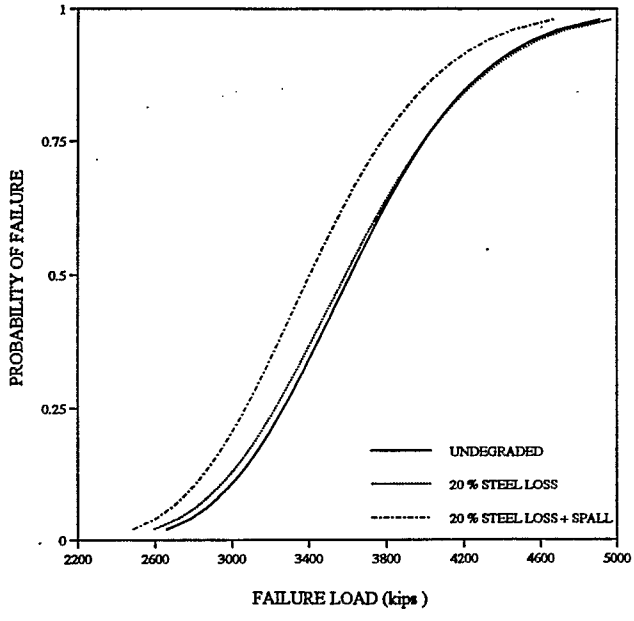

Fig. 8 Fragility Curves for Example Shear Wall (1 kip = 4.45 kN)